Title	Poleward eddy-induced warm water transport across a shelf break off Totten Ice Shelf, East Antarctica
Authors	Daisuke Hirano, Kohei Mizobata, Hiroko Sasaki, Hiroto Murase, Takeshi Tamura, Shigeru Aoki
Citation	Communications Earth & Environment, 2(153), 1-8, 2021
Issue Date	2021-8-6
Type	Journal Article
URL	https://doi.org/10.1038/s43247-021-00217-4
Right	
Textversion	publisher

Poleward eddy-induced warm water transport across a shelf break off Totten Ice Shelf, East Antarctica

Daisuke Hirano[1,2,3,4 ✉], Kohei Mizobata [5], Hiroko Sasaki[6], Hiroto Murase [5], Takeshi Tamura[3,4] & Shigeru Aoki[1]

Ice mass loss in the Wilkes Land sector of East Antarctica and the Amundsen and Bellingshausen Sea sectors of West Antarctica has contributed to a rise in sea levels over several decades. The massive continental ice behind the Totten Ice Shelf, equivalent to a few meters of sea-level rise, is grounded well below sea level and therefore, potentially vulnerable to oceanic heat. Here, we present analyses of comprehensive hydrographic observations at the continental slope and shelf break regions off Totten Ice Shelf. We provide robust evidence that the relatively warm Circumpolar Deep Water that originates at intermediate depths in the Antarctic Circumpolar Current is transported efficiently towards the shelf break by multiple cyclonic eddies. We propose that these semi-permanent cyclonic circulations play a critical role in transporting the available ocean heat towards Totten Ice Shelf, and melting it from underneath, thus eventually influencing the global climate.

[1] Institute of Low Temperature Science, Hokkaido University, Sapporo, Japan. [2] Arctic Research Center, Hokkaido University, Sapporo, Japan. [3] National Institute of Polar Research, Tachikawa, Japan. [4] The Graduate University for Advanced Studies, Tachikawa, Japan. [5] Tokyo University of Marine Science and Technology, Tokyo, Japan. [6] Japan Fisheries Research and Education Agency, Yokohama, Japan. ✉email: hirano.daisuke@nipr.ac.jp

A recent study has demonstrated that the mass loss of the Antarctic Ice Sheet was not only in the Amundsen and the Bellingshausen Sea sectors of West Antarctica but also in the Wilkes Land sector of East Antarctica[1]. A study noted that the Wilkes Land sector of East Antarctica has been a significant contributor to sea-level rise over the last 40 years. In East Antarctica, the largest ice discharge occurs through the Totten Glacier from the Aurora Subglacial Basin in Wilkes Land, grounded below sea level[2] (Fig. 1a). This basin is characterized as a region potentially vulnerable to ocean thermal forcing in East Antarctica because of its marine-based ice condition[3,4]. The expansive ice in the Aurora Subglacial Basin behind the Totten Glacier would be equivalent to a >3.5 m rise in sea level[5,6]. Compared to other East Antarctic ice shelves, the highest area-averaged basal melt rate is estimated for the Totten Ice Shelf (hereafter TIS, 10.5 ± 0.7 m yr^{-1})[7]. In the Southern Ocean, the strongest source of oceanic thermal forcing is the warm Circumpolar Deep Water (CDW), originating from intermediate depths in the offshore Antarctic Circumpolar Current (ACC) region[8]. Increased mass loss from the West Antarctic Ice Sheet is principally driven by an increase in basal melting of the Amundsen and the Bellingshausen Sea ice shelves by the strengthening of warm CDW inflows[9,10]. CDW inflow across the shelf break is a crucial process controlling the mass balance for ice shelves/sheets and therefore, it eventually influences the Antarctic as well as global climate.

While the continental shelf in East Antarctica is typically occupied by cold waters[11], recent hydrographic observations revealed warm modified CDW (mCDW) inflows at ice fronts of the TIS ($\sim -0.4\,°C$)[12] and Shirase Glacier Tongue (>0 °C)[13], consistent with satellite-derived high basal melt rates for these regions[7]. These are considered as firm observational evidence of the warm ocean–cryosphere interaction beneath the floating ice shelf (and ice tongue), which is atypical in East Antarctica. The limited historical hydrographic observations around the shelf break off TIS[14–17] suggested that bathymetric features control the across-slope transport of offshore-origin mCDW and depression with a bottom depth deeper than 500 m (Fig. 1b, c) is required for "bathymetric-controlled" mCDW transport. Further, integrated data from Ice Argo floats, hydrographic profiling by seals, and numerical modeling showed the seasonality in the pathway and water properties of mCDW inflows into the depression[17]. However, we do not thoroughly understand mCDW transport from offshore ACC to the continental slope of the focal region, which is strongly associated with the available oceanic heat flux for continental ice melting. Although poleward transport of offshore-origin warm CDW plays a critical role in regulating the available ocean heat for melting continental ice, specific knowledge of ocean heat transport from offshore toward the TIS cavity is lacking.

Most recently, Mizobata et al.[18] have provided important suggestions for poleward CDW transport toward TIS along the Sabrina Coast. Using satellite altimeter data, they constructed a spatio-temporally high-resolution dataset for dynamic ocean topography (DOT) over the Southern Ocean, north of shelf break (details in the "Methods" section). The DOT data unveiled a complete picture of an eddy train consisting of four quasi-stational cyclonic eddies with a spatial scale of ~100–200 km (Fig. 2); this was partially observed by a previous study[19]. Hydrographic profiles and mooring data revealed that the barotropic current structure in the Vincennes Eddy off Knox and Budd Coasts transports offshore warm water poleward and cold Antarctic Bottom Water equatorward at the eddy's eastern and western limbs, respectively. However, poleward CDW transport induced by cyclonic eddies is only verified for the Vincennes Eddy west of TIS[18]. Therefore, we can only speculate regarding such CDW
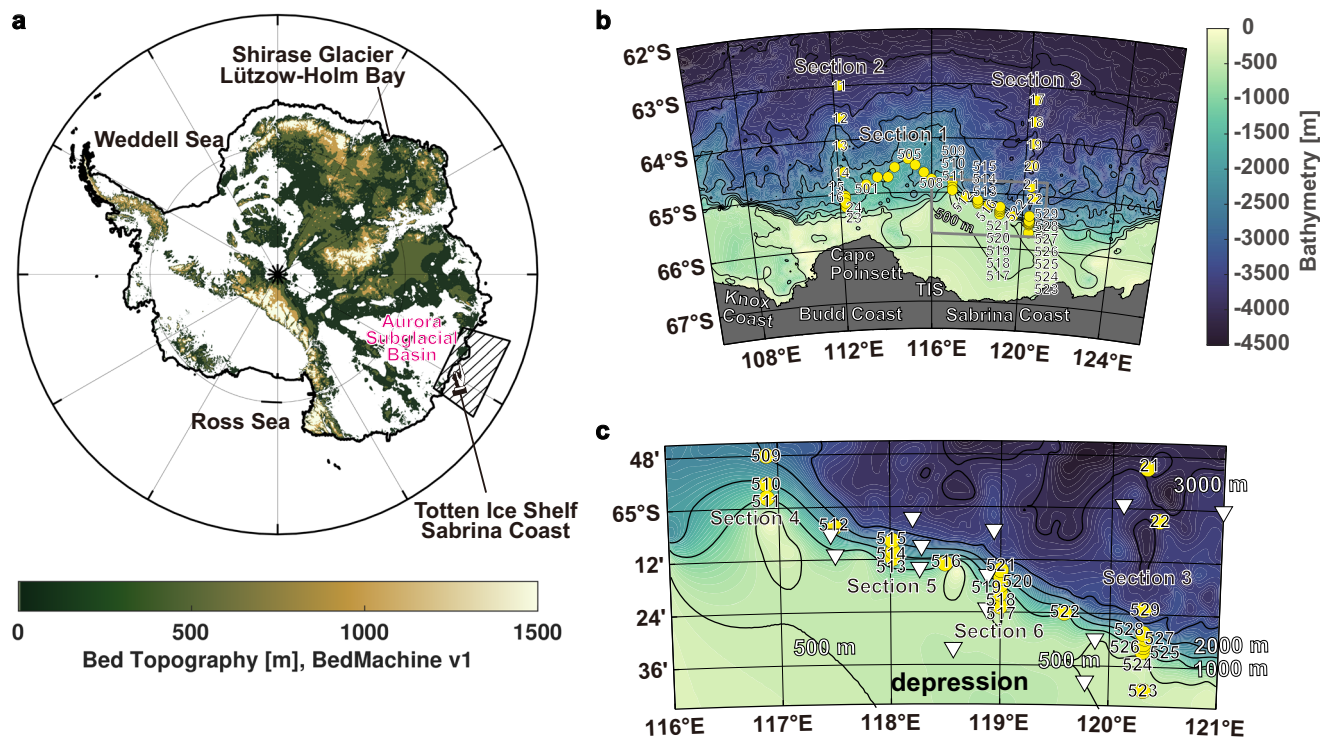

Fig. 1 Study area off Totten Ice Shelf, East Antarctica. a The latest bed topography over the Antarctic Continent from the BedMachine Antarctica v1[3]. The hatched region is our study area off Totten Ice Shelf (TIS) on the Sabrina Coast, East Antarctica. **b** Bathymetry map of our study area based on the International Bathymetric Chart of the Southern Ocean (IBCSO)[33], where the domain is indicated by the hatched region in (**a**). Yellow circles represent the positions of comprehensive and closely spaced conductivity–temperature–depth (CTD) stations by R/V *Kaiyo-Maru*. **c** Detailed bathymetry map from shelf break to continental slope regions, where the domain is indicated by the enclosed region in (**b**). In addition to the *Kaiyo-Maru* CTD stations (yellow circles), the positions of CTD stations by RVIB *NB Palmer* in 2015[16] are also shown as white inverted triangles.
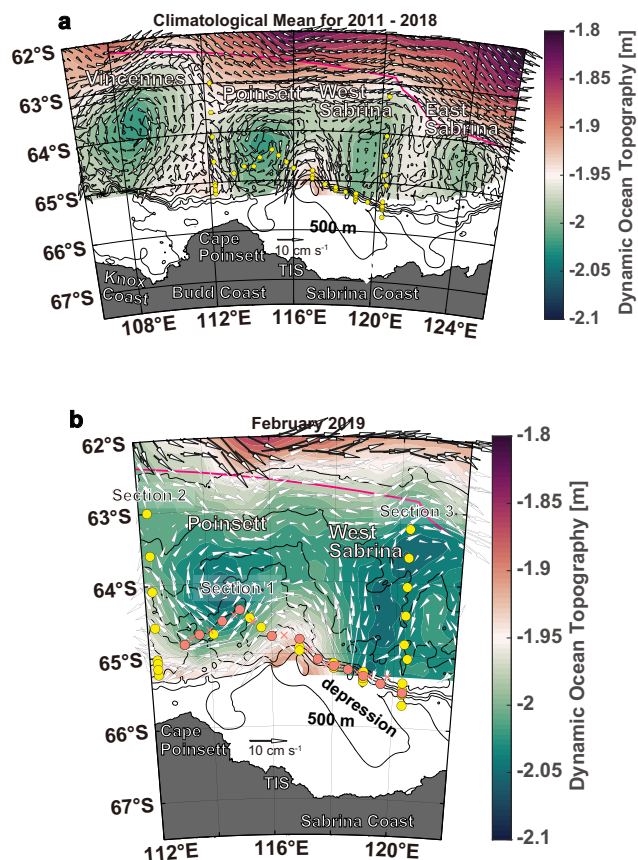
Fig. 2 Multiple cyclonic eddies off Knox, Budd, and Sabrina Coasts.
Spatial distributions of satellite-derived dynamic ocean topography (DOT,
color) and surface velocity (vector). **a** Climatological mean for 2011–2018
and **b** February 2019 (corresponding to the period of the
conductivity–temperature–depth (CTD) observations at Sta. 501–529).
Yellow circles represent the positions of CTD stations. Orange circles
indicate the positions of hydrographic profiles used for absolute velocity
calculations (Fig. 3d), while orange crosses are the grids for the referenced
DOT-derived surface velocity in the calculations. The pink line represents
the southern boundary of the Antarctic Circumpolar Current[8]. From west to
east, cyclonic eddies comprising the "eddy train" are the Vincennes Eddy,
Poinsett Eddy, West-Sabrina Eddy, and East-Sabrina Eddy[18].

transport by the Poinsett and West-Sabrina Eddies off the Sabrina
Coast (Fig. 2), which may be responsible for the ocean heat transport
that would be associated with the melting of TIS from below. In other
words, estimating the stability of the large marine-based ice sheet
behind TIS requires the determination of eddy contributions to
poleward ocean heat transport based on in-situ observations.

To explore the availability of ocean heat transport for TIS
melting, we carried out closely spaced hydrographic observations
at the continental slope and the shelf break regions (see the
"Methods" section; Fig. 1). Combined with the satellite-derived
ocean circulation data (see the "Methods" section; Fig. 2), we
demonstrated that quasi-stational cyclonic eddies found off the
Sabrina Coast play a critical role in poleward CDW transport,
which is one of the presumable upstream determinants of the
ocean heat flux into the TIS sub-ice cavity.

Results
CDW distribution at continental slope and shelf break regions.
To describe water mass distribution, we defined hydrographic

sections (Fig. 1b, c; described in the "Methods" section). Subsurface
water with warm temperature (>1 °C), high salinity (>34.7), and low
dissolved oxygen (DO) content (<210 μmol kg⁻¹), termed as
mCDW, is observed at depths ~300–500 dbar along the upper con-
tinental slope off TIS (113–121°E, zonal Section 1, Fig. 3). The
mCDW spatial distribution is worthy of special mention considering
remarkably warm cores (1.2–1.4 °C) at 350–400 dbar that are spa-
tially scattered rather than continuous, wherein the mCDW is
notably thick in the vertical extent (Stations [hereafter, Sta.] 502, 507,
512, and 522, Fig. 3a). The mCDW cores observed in February 2019
were at much higher temperatures than the warmer intrusion of
mCDW previously observed from March to June on the upper slope
(warmer than 0 °C, but mostly cooler than 1 °C)[17]. A positional
correspondence between eddies and warm cores is defined by the
that particularly warm waters are consistently observed around the
eastern sides of the cyclonic Poinsett (Sta. 507) and West-Sabrina
(Sta. 522) Eddies (Figs. 2b, 3a). We further note that warm cores are
also located on the western side of the Poinsett (Sta. 502) and West-
Sabrina (Sta. 512) Eddies (Figs. 2b, 3a). It is worth highlighting that
similar correspondence is determined for the East-Sabrina Eddy,
demonstrated by the expendable conductivity–temperature–depth
(XCTD) observations across the southern part of this eddy (Sup-
plementary Fig. 1). The in-situ observational pieces of evidence for
Poinsett, West-Sabrina, and East-Sabrina Eddies (this study), as well
as Vincennes Eddy[18], firmly represent a robust correspondence
relationship between the locations of eddies and warm cores. Fur-
thermore, semi-permanent features of the Poinsett and West-Sabrina
Eddies and corresponding warm water transport at the eddy's east-
ern/western edges are confirmed based on the hydrographic obser-
vations from icebreaker *Shirase* in December 2019 (Supplementary
Fig. 2) and February 2020 (Supplementary Fig. 3).

Poleward CDW transport induced by eddies. Subsequently, we
focus on the possibility of the poleward transport of offshore
warm waters induced by an eddy. Figure 4 shows meridional
water mass distributions at the western limb of Poinsett Eddy
(Section 2) and eastern limb of West-Sabrina Eddy (Section 3),
respectively, corresponding to northward and southward flowing
regions (Fig. 2). Although these sections do not belong to the
same eddy, the distinct difference in meridional extensions of
offshore warm water is well-demonstrated by isotherms of
1.0–1.6 °C (white contours in Fig. 4a, d) at the western and
eastern limbs of the cyclonic eddies. The warmer water is present
much closer to the upper continental slope at the eastern limb
(~1 °C, Fig. 4d) than at the western limb (0.6–0.8 °C, Fig. 4a),
suggesting that a southward current of the cyclonic eddy is
associated with a warmer mCDW.

To verify the role of eddies in CDW transport, we now
consider the absolute velocity (see the "Methods" section; Fig. 3d)
estimated from a combination of the CTD-derived geostrophic
velocity and the DOT-derived surface velocity (Fig. 2b). The
almost barotropic structures, comprising alternate northward and
southward currents, are evident along the continental slope,
representing an eddy-like feature. As suggested from the spatial
pattern of warm cores (Fig. 3a), both southward and northward
currents bring the warm cores along the eastern and western sides
of eddies, respectively (Fig. 3d), providing strong evidence to
demonstrate the meridional mCDW transport by eddies.

Below the thick cold Winter Water layer (~−1.8 °C near the
freezing point), thin layers of warm mCDW (0.57–0.99 °C) are
present near the seafloor of the shelf break (bottom depths of
437–596 m) around the eastern half of West-Sabrina Eddy
(Section 6 and southern part of Section 3, Fig. 5e–h), indicating
the inflow of offshore-origin mCDW across the upper continental
slope onto the shelf break. On the other hand, the warm cores
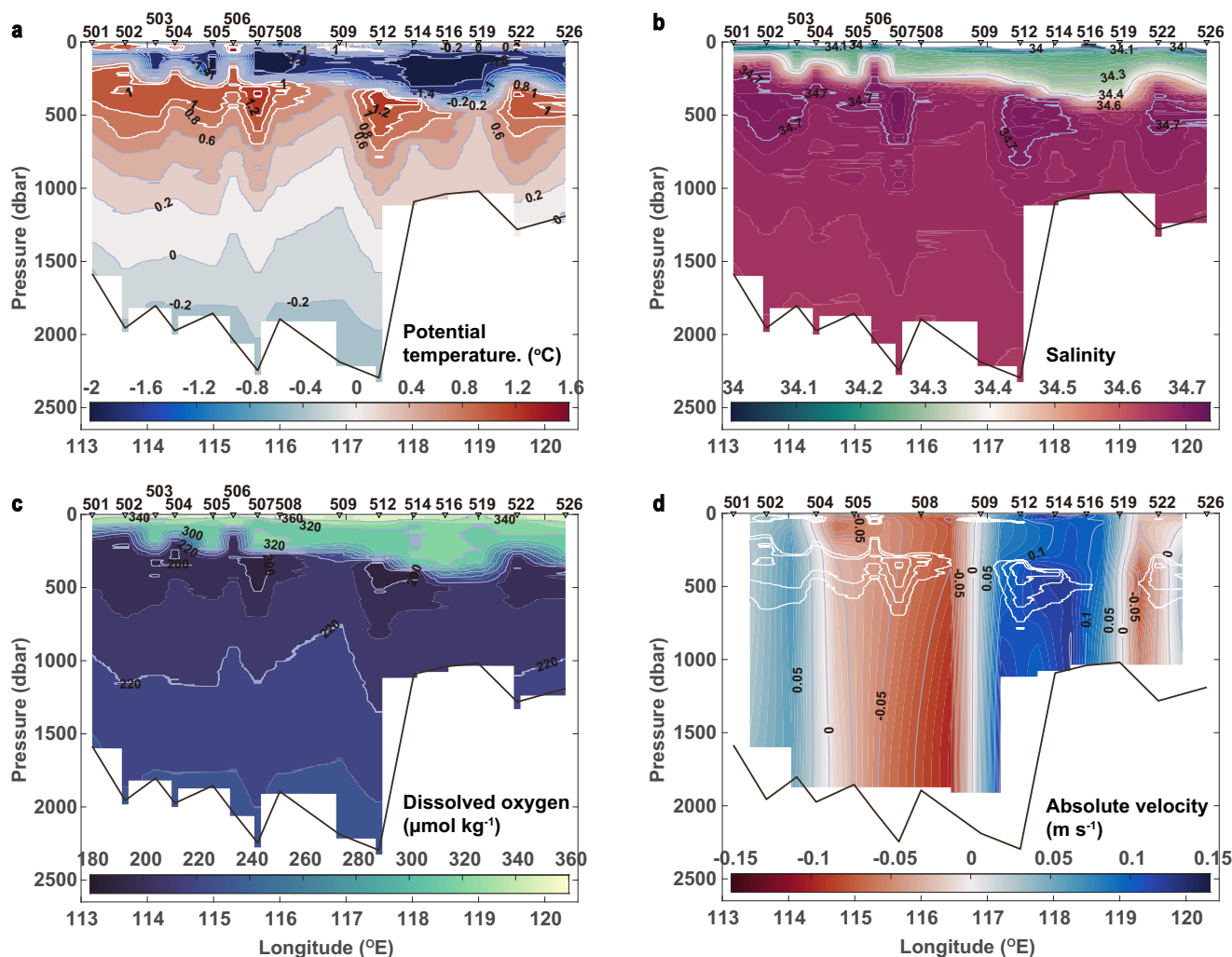
Fig. 3 Poleward eddy-induced warm water transport, toward the shelf break. Zonal hydrographic sections of **a** potntial temperature (°C), **b** salinity, **c** dissolved oxygen (µmol kg⁻¹), and **d** northward absolute velocity (m s⁻¹) along the continental slope (Section 1). In panels **a** and **d**, warm cores with potential temperatures higher than 0.8 °C are highlighted in white.

observed around the western half of West-Sabrina Eddy are located at the southernmost (Section 4, Fig. 5a, b) and intermediate (Section 5, Fig. 5c, d) parts of the meridional sections (locations of warm cores shown by arrows in Fig. 5a, c), although warmer (with lower DO) waters of CDW-origin are generally found in the offshore region. This demonstrates an entirely different aspect of the meridional warm core distribution from that observed at the eastern limbs (Fig. 5e–h). Inflows of warm mCDW have been previously observed from the shelf break to depression regions with depths of 400 m or more, in the summer of 1996 (BROKE)[14], late winter of 2001 (SIPEX)[15], autumn of 2015 (NBP2015 Cruise)[16], and throughout the year (Ice Argo Float)[17]. The results from historical observations as well as those from this study indicate that mCDW inflows onto the shelf break are not intermittent but continuously occur along with seasonal variability.

Hydrographic profiles and mooring data have confirmed that the velocity structure of Vincennes Eddy (Fig. 2a) is almost barotropic[18]. In addition, our estimate for the absolute velocity field across Poinsett to West-Sabrina Eddies showcases the nearly barotropic structure of the meridional velocity component (Fig. 3d). Accordingly, it is reasonable to consider that the DOT-derived surface velocities (vectors in Fig. 2) partially represent the ocean circulation in the intermediate depths of

the mCDW layer. The apparent difference in the meridional distribution of warm mCDW at the eastern and western limbs of the cyclonic eddies (Figs. 3–5) indicates the efficient poleward mCDW transport by Poinsett and West-Sabrina Eddies. Based on the above observational findings, we determine a unique plausible circulation pattern of offshore warm mCDW, comprising inflows at the eastern limb of the cyclonic eddies and return flows at the western limbs of a part of mCDW once transported onto the shelf break. In other words, the findings strongly suggest that not all ocean heat transported across the shelf break is available for the basal melting of TIS on the Sabrina Coast.

Discussion

Combined with the satellite-derived DOT dataset covering sea ice areas[18], the new closely spaced hydrographic profiles have demonstrated that multiple cyclonic eddies off the Sabrina Coast contribute to efficient poleward transport of offshore-origin warm mCDW. It should be noted that the mesoscale eddies (typically with a spatial scale of the order of few tens of kilometers), including a form of anti-cyclonic warm-core eddies, also contribute to the poleward heat transport across/from the ACC region[20–22], but the DOT dataset's spatiotemporal resolution (monthly mean with 0.2° × 0.2° grid spacing) is insufficient for capturing such mesoscale processes. The
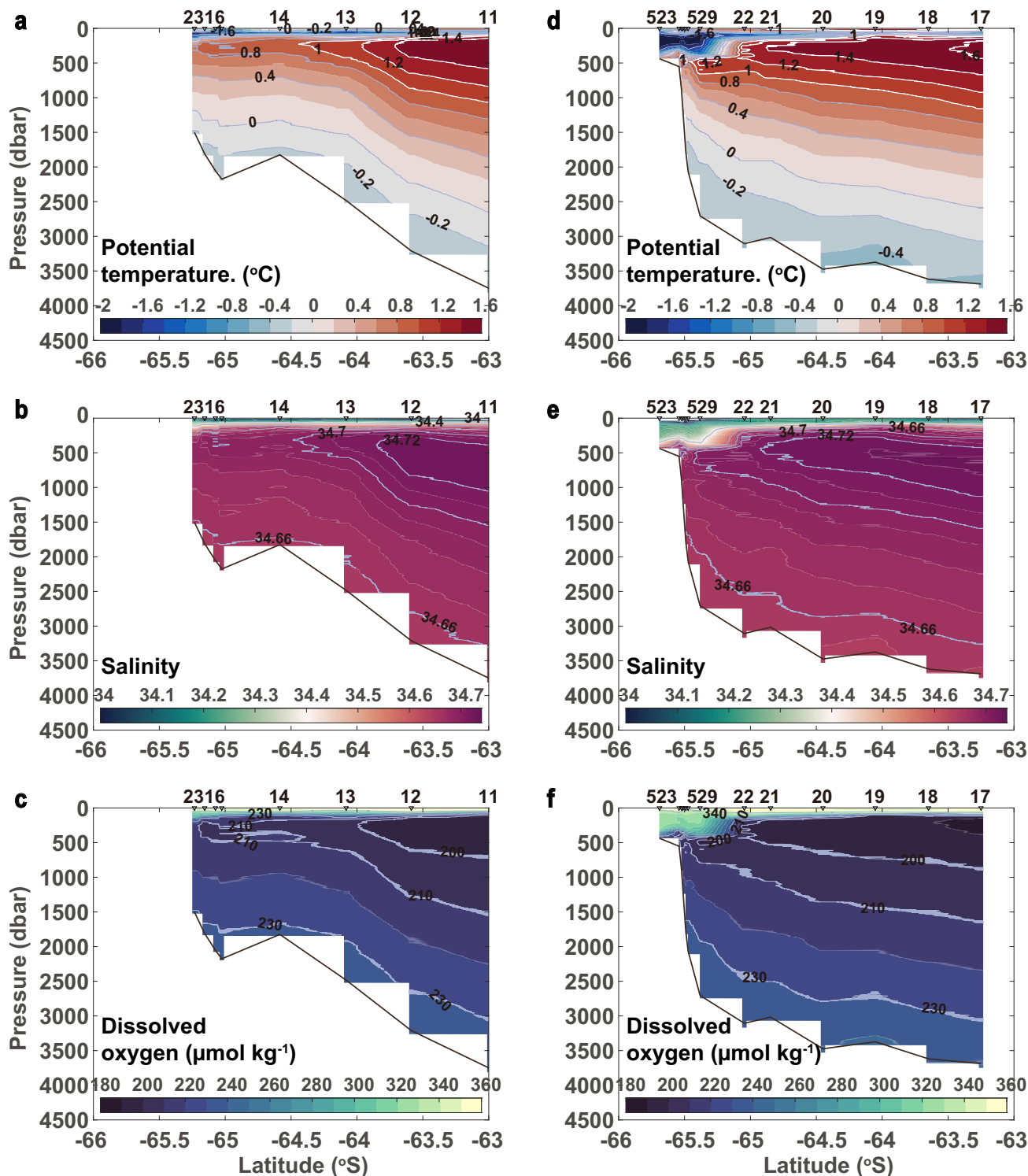
Fig. 4 Meridional warm water distribution at eddy's eastern/western edges. Meridional sections along the western (Section 2, panels **a**–**c**) and eastern (Section 3, panels **d**–**f**) limbs of the cyclonic eddies. **a**, **d** Potential temperature (°C), **b**, **e** salinity, and **c**, **f** dissolved oxygen (μmol kg⁻¹). In panels **a** and **d**, potential temperatures warmer than 1 °C are highlighted with white contours. Note that the observation dates of Section 3 stations were set apart: Sta. 17–22 (early January 2019) and Sta. 523–529 (late February 2019).

bathymetric depression just south of the shelf break has a depth of ~500 m and a width of ~190 km (Fig. 1), enabling southward access of mCDW onto the continental shelf (i.e., the bathymetric-controlled mCDW intrusions)[16,17]. Note that the bathymetric features of the depression based on the International Bathymetric Chart of the Southern Ocean (IBCSO) data is oversimplified than realistic

demonstrated by the multibeam bathymetric data[23]. Furthermore, results from Ice Argo Float, seal-mounted CTD, and numerical modeling posited seasonal variations in inflow paths and water properties of mCDW[17]. In autumn, warmer mCDW flows into the depression from the east following the westward Antarctic Slope Current (ASC), whereas in other seasons, the opposite occurs
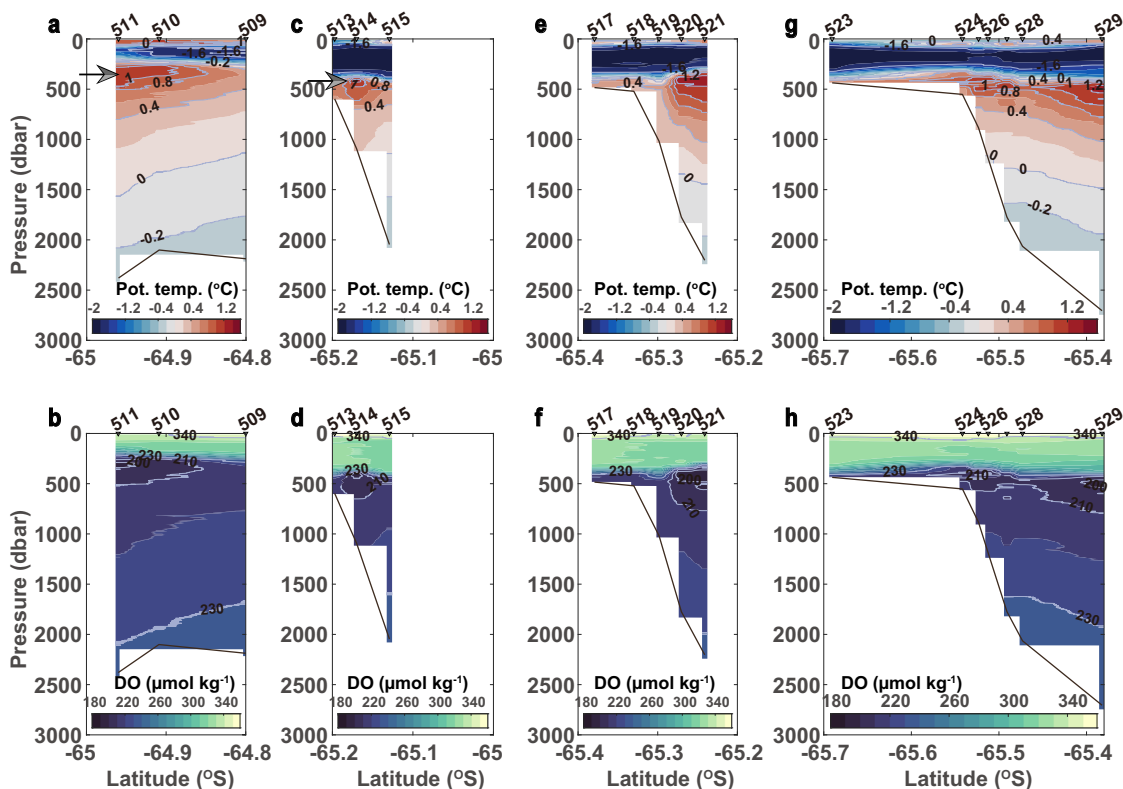
Fig. 5 Warm water distribution from upper slope across shelf break. Closely spaced meridional sections of potential temperature (°C) and dissolved oxygen (µmol kg⁻¹) from upper continental slope to shelf break regions at **a**, **b** Section 4, **c**, **d** Section 5, **e**, **f** Section 6, and **g**, **h** southern part of Section 3. Arrows in panels **a** and **c** represent the locations of warm cores observed around the western half of the West-Sabrina Eddy.

following an eastward undercurrent carrying relatively cold mCDW[17]. Further, the mCDW inflow paths from east or west of the depression can be consistently linked to the mCDW circulation from the ACC to the upper slope region via eddy-induced transport by the quasi-stational Poinsett and West-Sabrina Eddies (Figs. 2–5). Thus, the warm mCDW circulation from offshore ACC (source) to the shelf break appears akin to an intricate "highway junction" with some fueling stations provided by multiple eddies off TIS on the Sabrina Coast of Wilkes Land, East Antarctica.

Here, we estimate eddy-induced heat transport by Poinsett and West-Sabrina Eddies (details mentioned in the "Methods" section). Poleward heat transports of 11.7 TW by Poinsett Eddy and 2.6 TW by West-Sabrina Eddy are estimated; these are greater than the required heat transport of ~0.7 TW for basal melting beneath TIS (63.2 Gt yr⁻¹)[7]. These estimates suggest that semi-permanent off-shore cyclonic eddies transport sufficient oceanic heat for the TIS basal mass loss toward the shelf break. However, caution should be exercised in interpreting this estimation. The near-seafloor mCDW temperature is 0.5–1 °C at the shelf break (Sta. 517–518, Fig. 5e; Sta. 523–524, Fig. 5g), whereas it is −0.5 to −0.4 °C at the TIS ice front[12]. This notable decrease in water temperature strongly suggests the involvement of water-mass alteration processes, such as mixing with overlying cold Winter Water or heat loss by deep convection associated with sea-ice production in Dalton Polynya, during on-shelf circulation across the shelf break to the TIS ice front. Further, certain amount of the mCDW, once transported across the shelf break, might return offshore (Fig. 5a–d) without being transported beneath the TIS. This suggests that eddy-induced poleward ocean heat delivery across the shelf break is redistributed by the on-shelf water-mass alternation and circulation, determining the amount of the subsequent ocean heat transport beneath TIS.

Observational and numerical model studies have pointed out that "eddies" play crucial roles in the cross-slope exchange associated with heat transport toward ice shelves[24–26]. For example, in the Eastern Weddell Sea, an eddy-driven overturning is enhanced, especially under weak alongshore winds, resulting in warm water transport across the shelf break toward the Fimbul Ice Shelf[24]. However, the spatial scale of such eddy overturning is much smaller than that of cyclonic eddies off the Sabrina Coast (Fig. 2). Inter-estingly, our closely spaced profiles also show a discontinuous distribution of warm water near the seafloor at the eastern sides of Poinsett and West-Sabrina Eddies (Section 6 and the southern part of Section 3, Fig. 5e–h), suggesting an eddy-driven overturning as in the Eastern Weddell Sea. This further suggests that larger cyclonic eddies carry mCDW from the offshore ACC to the upper slope region, and a part of these might subsequently cross the shelf break with the assistance of smaller eddies. The direct contribution of cyclonic eddies (including smaller eddy overturning) to the cross-slope transport of warm water is still unclear, specifically the extent of merging of mCDW with the westward ASC or eastward undercurrent after it arrives at the upper continental slope. A high-resolution mooring array across the upper slope to the shelf break regions is desired to quantify the contributions to the mCDW transport from various-scale eddies, slope jets (ASC and under-current), and bathymetric features (and their interactions).

Even at almost the same locations (Sta. 507 and 522 at the eastern limbs of Poinsett and West-Sabrina Eddies, respectively), we observe warmer mCDW (>1–1.2 °C) than those that were previously found on the western (at 115–116°E and ~65°S) and eastern (at 119–120°E and ~65.5°S) upper slopes north of the depression[17]. Some possible factors in determining the mCDW properties of the continental slope region are the positions and magnitudes of wind-driven upwelling[27], cyclonic eddy train[18,19]

(Fig. 2), and eddy overturning[24]. Moreover, the presence of warm cores is highly localized along the continental slope (e.g., the horizontal scale of the warm core centered at Sta. 507 is quite small, Fig. 3a). In other words, this might lead to misinterpretation of a "visible" difference in the mCDW properties and distribution if the spatial resolution of the profiles is coarse. Thus, the locality of warm cores (Fig. 3) indicates the necessity of closely spaced hydrographic observations to capture the poleward eddy-induced transport of warm mCDW that would control the rate of basal melting beneath the ice shelves along the Sabrina Coast.

At present, a reliable DOT dataset for the south of the shelf break has not been constructed due to the low availability of radar signals from the sea surface. Therefore, the satellite-derived DOT cannot provide any information regarding on-shelf mCDW circulation toward the TIS cavity. Comprehensive hydrographic and bathymetric surveys across the continental shelf are indispensable for elucidating the mCDW circulation regulating the ocean heat flux for TIS basal melting. Further, identifying mCDW modification processes over the Sabrina Coast's continental shelf, such as sea-ice production accompanied by seasonal deepening of the overlying cold water layer that would modify the mCDW thickness in the Dalton Polynya (~120°E), east of TIS, is also important to quantitatively evaluate the variability of available oceanic heat flux beneath the TIS cavity. Further accumulation of observational findings from the offshore ACC to the TIS ice front regions are useful in validating and improving the numerical modeling framework. This also contributes to improving the accuracy of future prediction of changes in the East Antarctic ice sheet mass balance, which contains a large mass of continental ice[3,4], and the associated sea level rise.

The Amundsen and the Bellingshausen Sea ice shelves in West Antarctica are most susceptible to the ocean heat flux that results from CDW inflows[8,28,29] as ACC transporting warm CDW approaches the shelf break. Instead, this study posits that offshore cyclonic eddies play a critical role in efficient poleward transport of warm water toward TIS on the Sabrina Coast as in the case of the cyclonic Weddell Gyre that transports warm water toward the Shirase Glacier Tongue with a high basal melt rate[7,13]. This strongly suggests that the presence of such cyclonic circulations is a characteristic of the offshore setting for creating warm on-shelf ocean conditions and associated high basal melt rates in the East Antarctic continental margin, typically occupied by cold waters[11], and eventually influence the Antarctic and global climate. This study proposes that poleward eddy-induced transport of offshore-origin warm water plays a critical role in regulating the available ocean heat for melting East Antarctic continental ice from underneath.

Methods

Comprehensive in-situ hydrographic observations off Totten Ice Shelf on the Sabrina Coast. In December 2018 and January and February 2019, we carried out comprehensive hydrographic observations off TIS on the Sabrina Coast in East Antarctica (Fig. 1), under the research project led by the Fisheries Agency of Japan—"multidisciplinary ecosystem survey in the eastern Indian sector of the Antarctic (CCAMLR Division 58.4.1) with a focus on Antarctic Krill"[30]. We successfully obtained high-accuracy vertical profiles of temperature, salinity, and DO from the surface to ~10 m above the bottom using the SBE 9plus conductivity–temperature–depth profiler (CTD, Sea-Bird Electronics, Washington State, USA) and RINKO DO profiler (JFE Advantech, Hyogo, Japan). The observation data satisfy the requirement of Global Ocean Ship-based Hydrographic Investigations Program (GO-SHIP)[31] standard accuracies (0.002 °C for temperature, 0.002 for salinity, and 1% for DO). From the shelf break to the upper slope regions, we obtained high spatial resolution profiles (Sta. 501–529 at 29 stations), compared with historical ship-based observations[16] (white inverted triangles in Fig. 1c). The closely spaced hydrographic profiles allow for detailed investigation of images of distribution and poleward transport of offshore-origin CDW that would contribute to the melting of TIS. In addition, two meridional sections along 112°15′E and 120° 19′E are the revisit observation sections of Baseline Research on Oceanography, Krill and the Environment (BROKE) in 1996[14].

To describe water mass distribution, we define hydrographic sections (Fig. 1b, c) as follows; Section 1: zonal section along the continental slope with a bottom depth of ~1000–2000 m (Sta. 501–509, 512, 514, 516, 519, 522, 526), Section 2: meridional section along ~112°15′E (BROKE revisit section), Section 3: meridional section along ~120°19′E (BROKE revisit section), and Sections 4–6: closely spaced meridional sections across the shelf break and upper slope regions (from west to east, Sta. 511–509, 513–515, and 517–521).

Satellite-derived dynamic ocean topography (DOT)[18]. We utilize a monthly mean dataset of 0.2° × 0.2° DOT over the Southern Ocean (except for regions shallower than ~1000 m; Fig. 2), derived from satellite altimeter data[18] (from January 2011 to April 2019; for this study, the data period is now extended to February 2020, Supplementary Figs. 2 and 3), to explore the characteristics of ocean circulation, especially eddy fields, associated with poleward CDW transport. This DOT dataset is spatially seamless even in sea-ice covered regions and hence, we can estimate DOT-derived geostrophic velocity at the ocean surface irrespective of the presence of sea ice (vectors in Fig. 2). Using the DOT dataset, Mizobata et al.[18] revealed an "eddy train" consisting of four cyclonic eddies—Vincennes Eddy, Poinsett Eddy, West-Sabrina Eddy, and East-Sabrina Eddy (Fig. 2a). Spatial scales and mean positions of the four cyclonic eddies are 240 × 220 km centered at 109°E and 63.8°S for Vincennes Eddy, 195 × 170 km centered at 115°E, and 64.5°S for Poinsett Eddy, 140 × 220 km centered at 119.5°E and 64.5°S for West-Sabrina Eddy, and 140 × 100 km centered at 124°E and 64.8°S for East-Sabrina Eddy. Section 1 zonally covers two eddies—Poinsett Eddy and West-Sabrina Eddy, and Sections 2 and 3 correspond to the western (i.e., northward flowing region) and eastern (i.e., southward flowing region) limbs of the Poinsett and West-Sabrina Eddies, respectively (yellow circles, Fig. 2). Mizobata et al.[18] conducted hydrographic observations to capture the detailed structure and characteristics of the Vincennes Eddy, while our new observations exhaustively cover the two cyclonic eddies that would relate to the heat transport available for the melting of TIS sub-ice cavity (yellow circles, Fig. 2).

Calculation of absolute velocity from hydrographic and satellite-derived DOT data. The DOT is the sum of the baroclinic (steric) and the barotropic (including tidal component, i.e., bottom pressure term) components. As a result, DOT-derived velocity includes both baroclinic and barotropic components, but it can only be obtained at the sea surface. Using CTD measurements, the vertical profile of geostrophic velocity is obtained; however, only the baroclinic component is reflected in the profile. Note that a tidal correction (FES2004)[32] is applied to the sea surface height before obtaining the DOT[18], and therefore, tides may not alias the absolute velocity calculation. To obtain the vertical profiles of absolute velocity including baroclinic and barotropic components, the entire profile of geostrophic velocity calculated from CTD measurements is shifted such that the surface velocity matches the DOT-derived velocity. In this study, we determined the DOT-derived velocity for the location closest to where the geostrophic velocity was calculated (Fig. 2b); the range for determining the DOT-derived velocity was 0.1°. However, since the location between Sta. 522 and Sta. 526 is in the shallow region away from where DOT can be obtained, the search range is changed to 0.2°.

Estimation of eddy-induced poleward heat transport. Using along-slope potential temperature (Fig. 3a) and absolute velocity (Fig. 3d) sections, we estimate poleward heat flux at the layer between 400 and 600 dbar of the Poinsett Eddy and West Sabrina Eddy regions, based on the depths of warm water occupation and the seafloor of the shelf break. Ocean heat flux is expressed as follows; $\int_A C_P \rho (\theta - \theta_{ref}) v dA$, where A is the cross-section area, C_P is the specific heat of seawater, ρ is the density of seawater, θ is the potential temperature, and v is the cross-section velocity. We set −1.9 °C as a reference potential temperature (θ_{ref}), which is approximately the freezing point of seawater.

Data availability

References

1. Rignot, E. et al. Four decades of Antarctic Ice Sheet mass balance from 1979–2017. *Proc. Natl. Acad. Sci. USA* **116**, 1095–1103 (2019).
2. Young, D. A. et al. A dynamic early East Antarctic Ice Sheet suggested by ice-covered fjord landscapes. *Nature* **474**, 72–75 (2011).

3. Morlighem, M. et al. Deep glacial troughs and stabilizing ridges unveiled beneath the margins of the Antarctic ice sheet. *Nat. Geosci.* **13**, 132–137 (2020).

4. Fretwell, P. et al. Bedmap2: improved ice bed, surface and thickness datasets for Antarctica. *Cryosphere* **7**, 375–393 (2013).

5. Li, X., Rignot, E., Morlighem, M., Mouginot, J. & Scheuchl, B. Grounding line retreat of Totten Glacier, East Antarctica, 1996 to 2013. *Geophys. Res. Lett.* **42**, 8049–8056 (2015).

6. Greenbaum, J. S. et al. Ocean access to a cavity beneath Totten Glacier in East Antarctica. *Nat. Geosci.* **8**, 294–298 (2015).

7. Rignot, E., Jacobs, S., Mouginot, J. & Scheuchl, B. Ice-shelf melting around Antarctica. *Science* **341**, 266–270 (2013).

8. Orsi, A. H., Whitworth, T. & Nowlin, W. D. On the meridional extent and fronts of the Antarctic Circumpolar Current. *Deep Sea Res. Part I* **42**, 641–673 (1995).

9. Pritchard, H. D. et al. Antarctic ice-sheet loss driven by basal melting of ice shelves. *Nature* **484**, 502–505 (2012).

10. Shepherd, A. Wingham, D. & Rignot, E. Warm ocean is eroding West Antarctic Ice Sheet. *Geophys. Res. Lett.* **31**, L23402 (2004).

11. Schmidtko, S., Heywood, K. J., Thompson, A. F. & Aoki, S. Multidecadal warming of Antarctic waters. *Science* **346**, 1227–1231 (2014).

12. Rintoul, S. R. et al. Ocean heat drives rapid basal melt of the Totten Ice Shelf. *Sci. Adv.* **2**, e1601610 (2016).

13. Hirano, D. et al. Strong ice-ocean interaction beneath Shirase Glacier Tongue in East Antarctica. *Nat. Commun.* **11**, 1–2 (2020).

14. Bindoff, N. L., Rosenberg, M. A. & Warner, M. J. On the circulation and water masses over the Antarctic continental slope and rise between 80 and 150 degrees E. *Deep Sea Res. Part II* **47**, 2299–2326 (2000).

15. Williams, G. D. et al. Late winter oceanography off the Sabrina and BANZARE coast (117-128 degrees E), East Antarctica. *Deep Sea Res. Part II* **58**, 1194–1210 (2011).

16. Nitsche, F. O. et al. Bathymetric control of warm ocean water access along the East Antarctic Margin. *Geophys. Res. Lett.* **44**, 8936–8944 (2017).

17. Silvano, A. et al. Seasonality of warm water intrusions onto the continental shelf near the Totten Glacier. *J. Geophys. Res.* **124**, 4272–4289 (2019).

18. Mizobata, K., Shimada, K., Aoki, S. & Kitade, Y. The Cyclonic Eddy Train in the Indian Ocean Sector of the Southern Ocean as Revealed by Satellite Radar Altimeters and In Situ Measurements. *J. Geophys. Res.* **125**, e2019JC015994 (2020).

19. Wakatsuchi, M., Ohshima, K. I., Hishida, M. & Naganobu, M. Observations of a street of cyclonic eddies in the Indian-Ocean Sector of the Antarctic Divergence. *J. Geophys. Res.* **99**, 20417–20426 (1994).

20. Ansorge, I. J. et al. Evidence of a southward eddy corridor in the South-West Indian ocean. *Deep Sea Res. Part II* **119**, 69–76 (2015).

21. Meredith, M. P. Understanding the structure of changes in the Southern Ocean eddy field. *Geophys. Res. Lett.* **43**, 5829–5832 (2016).

22. Gille, S. T., McKee, D. C. & Martinson, D. G. Temporal changes in the Antarctic Circumpolar Current implications for the Antarctic continental shelves. *Oceanography* **29**, 96–105 (2016).

23. Fernandez, R. et al. Past ice stream and ice sheet changes on the continental shelf off the Sabrina Coast, East Antarctica. *Geomorphology* **317**, 10–22 (2018).

24. Nøst, O. A. et al. Eddy overturning of the Antarctic Slope Front controls glacial melting in the Eastern Weddell Sea. *J. Geophys. Res.* **116**, C11014 (2011).

25. Hattermann, T., Smedsrud, L. H., Nost, O. A., Lilly, J. M. & Galton-Fenzi, B. K. Eddy-resolving simulations of the Fimbul Ice Shelf cavity circulation: basal melting and exchange with open ocean. *Ocean Model.* **82**, 28–44 (2014).

26. Thompson, A. F., Stewart, A. L., Spence, P. & Heywood, K. J. The Antarctic Slope Current in a changing climate. *Rev. Geophys.* **56**, 741–770 (2018).

27. Greene, C. A., Blankenship, D. D., Gwyther, D. E., Silvano, A. & van Wijk, E. Wind causes Totten Ice Shelf melt and acceleration. *Sci. Adv.* **3**, e1701681 (2017).

28. Nakayama, Y., Menemenlis, D., Zhang, H., Schodlok, M. & Rignot, E. Origin of circumpolar deep water intruding onto the Amundsen and Bellingshausen Sea continental shelves. *Nat. Commun.* **9**, 1–9 (2018).

29. Wahlin, A. K. et al. Some Implications of Ekman layer dynamics for cross-shelf exchange in the Amundsen Sea. *J. Phys. Oceanogr.* **42**, 1461–1474 (2012).

30. Murase, H. et al. Cruise report of multidisciplinary ecosystem survey in the eastern Indian sector of the Antarctic (CCAMLR Division 58.4.1) with a focus on Antarctic krill during 2018/19 season by the Japanese survey vessel, Kaiyo-maru. *WG-EMM-19/42* [available from the CCAMLR Secretariat] (2019).

31. Hood, E. M., Sabine, C. L. & Sloyan, B. M. *The GO-SHIP Repeat Hydrography Manual: A Collection of Expert Reports and Guidelines*, Version 1. IOCCP Report 14 ICPO Publication Series 134 http://www.go-ship.org/HydroMan. html (2010).

32. Lyard, F., Lefevre, F., Letellier, T. & Francis, O. Modelling the global ocean tides: modern insights from FES2004. *Ocean Dynam.* **56**, 394–415 (2006).

33. Arndt, J. E. et al. The International Bathymetric Chart of the Southern Ocean (IBCSO) Version 1.0—a new bathymetric compilation covering circum-Antarctic waters. *Geophys. Res. Lett.* **40**, 3111–3117 (2013).

Acknowledgements

Author contributions

D.H. conceived this study. D.H., H.S., and H.M. designed and conducted hydrographic observations on board R/V *Kaiyo-Maru*. T.T. and S.A. conducted hydrographic obser-vations on board icebreaker *Shirase*. D.H. and K.M. analyzed the hydrographic and satellite observation data. D.H., K.M., and S.A. wrote the paper, and all authors discussed the results and commented on the manuscript.

Competing interests

The authors declare no competing interests.

Additional information

Publisher's note Springer Nature remains neutral with regard to jurisdictional claims in published maps and institutional affiliations.